Reusable, Flyback Liquid Rocket Booster for the Space Shuttle

Mark G. Benton*
University of Maryland, College Park, Maryland

This paper outlines a preliminary design for an unmanned, reusable, flyback liquid rocket booster (LRB) as an evolutionary follow-on to the Shuttle solid rocket booster (SRB). Previous Shuttle liquid-propellant booster concepts are reviewed in order to gain insight into these designs. The operating costs, environmental impacts, and abort options of the SRB are discussed. The LRB flight profile and advantages of LRB use are discussed. The preliminary design for the LRB is outlined in detail using calculations and drawings. This design maximizes the use of existing hardware and proven technology to minimize cost and development time. The LRB design is presented as a more capable, more environmentally acceptable, and safer Shuttle booster.

Nomenclature

A = aspect ratio
a = lift slope $(\partial C_l/\partial\alpha)$
b = wing span
C_d = drag coefficient
C_l = lift coefficient
C_m = pitching moment coefficient
C_n = yawing moment coefficient
CG = longitudinal center of gravity
c = chord, specific fuel consumption
$\bar{c}$ = mean aerodynamic chord
D = drag
e = Oswald efficiency factor
g = acceleration of gravity
h = altitude, CG position in fraction of $\bar{c}$
h_n = neutral point position in fraction of $\bar{c}$
i = incidence angle
L = lift, liquid
l = moment arm from $\bar{c}/4$ to CG
M = Mach number, mass
R = range, displacement downrange
S = reference area
T = thrust
t = time, airfoil thickness
V = velocity, volume
W = weight
α = angle of attack
β = angle of sideslip
γ = flight-path angle from local horizontal
δ = rudder deflection angle
ϵ = downwash angle
θ = flight-path angle from the local vertical
ρ = freestream air density

Subscripts

b = base
c = canard, cruise
f = fuelage
o = at zero lift
r = required, rudder
v = vertical stabilizer
wb = wing-body combination
0 = initial condition
1 = final condition

Partial Derivatives

$C_{m\alpha}$ = pitching moment coefficient with respect to angle-of-attack change
$C_{n\beta}$ = yawing moment coefficient with respect to angle-of-sideslip change
$C_{n\delta}$ = yawing moment coefficient with respect to change in rudder deflection

Introduction

MANY different concepts for Space Shuttle boosters were examined both before and after the current solid rocket booster (SRB) was selected. Concerns about the Shuttle SRB include its operating cost, environmental impact, and safety. The objective of this paper is to introduce a more capable, more environmentally acceptable, and safer follow-on Shuttle booster that uses liquid propellants and returns to the launch site after each mission. This liquid rocket booster (LRB) design is a high-performance reusable booster that draws on previous design experience and maximizes the use of existing hardware and proven technology to minimize cost and development time.

Previous Shuttle Liquid-Propellant Booster Designs

Many Shuttle booster concepts were examined in the early 1970's before the current configuration was settled on. Before SRB's were chosen, two favored designs featured liquid-propellant boosters. The first design used a single, large, manned, flyback booster based on the Saturn V first stage with five F-1 engines burning RP-1 and LO_2 (Fig. 1). This design was rejected because although it had a low-recurring cost, it had a high development cost, and the baseline F-1 was not really reusable in the sense of the current Space Shuttle main engine (SSME). There were additional concerns about priorities in abort situations because both vehicles were manned (Ref. 1,

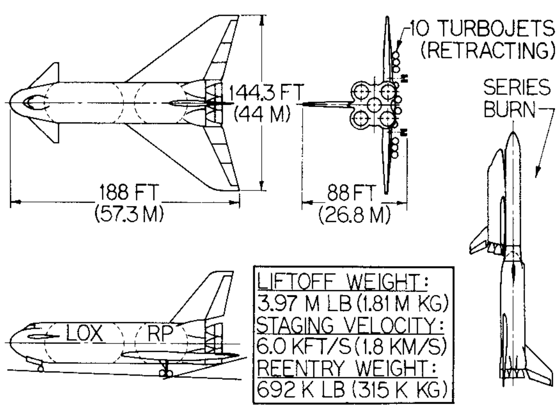

Fig. 1 1972 flyback booster concept.

Received April 25, 1988; revision received Jan. 21, 1989.

*Graduate Student, Minta-Martin Fellow, Department of Aerospace Engineering. Student Member AIAA.

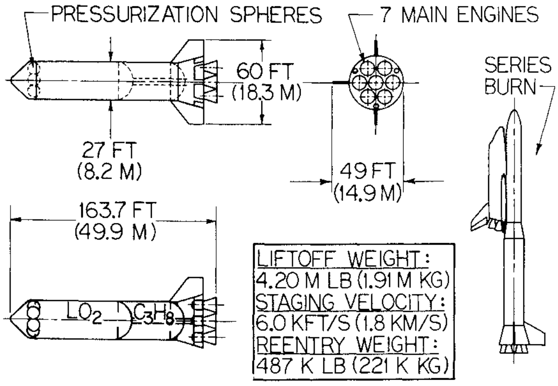

Fig. 2 1972 pressure-fed booster concept.

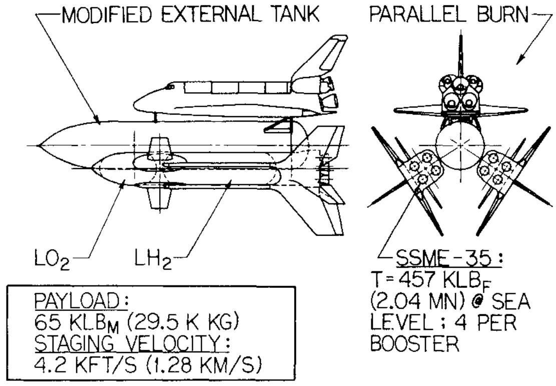

Fig. 4 1977 flyback booster concept.

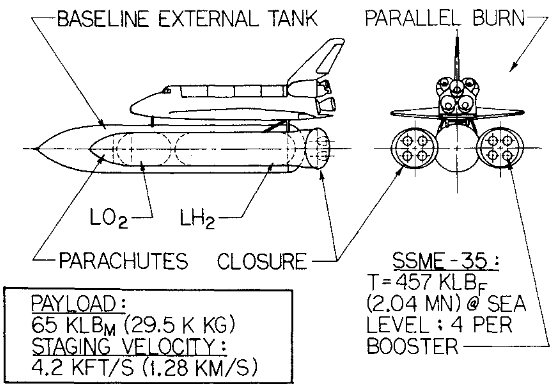

Fig. 3 1977 water-recovery booster concept.

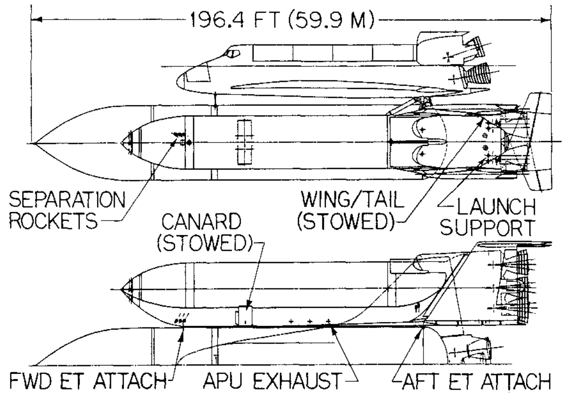

Fig. 5 LRB launch configuration, top and side views.

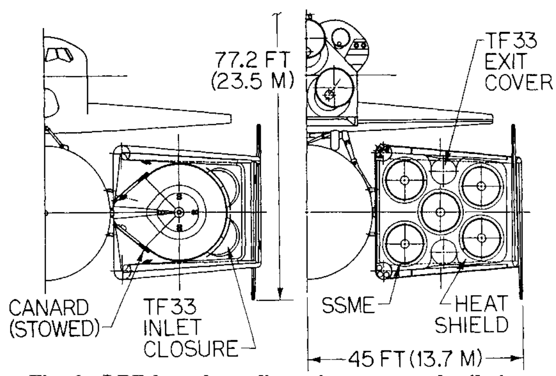

Fig. 6 LRB launch configuration, nose and tail views.

pp. 459–493). The second design used a single, large, liquid-propellant, pressure-fed booster (Fig. 2). This booster would be able to withstand ocean recovery because of its thick steel skin. This design was rejected because new, extremely large rocket engines and parachutes would have to be developed. Along with the high development costs, there were also concerns about engine reusability and seawater corrosion (Ref. 1, pp. 494–526).

The configuration finally selected, using the current SRB, had the lowest development cost but highest recurring cost (Ref. 1, pp. 832–838, and Ref. 2). The SRB's require elaborate, expensive infrastructure for postflight retrieval, propellant loading, and refurbishment. Concerns have been raised about the long-term use of the SRB because of its acidic exhaust plume that could damage the environment. In addition, solid-propellant boosters are difficult to extinguish once ignited, making abort separation of boosters, external tank (ET), and Orbiter difficult to accomplish before SRB burnout.

Several liquid-propellant booster concepts for the Shuttle were considered by NASA in the late 1970's. Two favored designs each featured a pair of strap-on boosters with four SSME derivative engines (SSME-35's) burning LH_2 and LO_2 per booster. The SSME-35 was a proposal to redesign the high-expansion-ratio SSME for higher thrust at low altitudes. The first design featured ocean recovery with a clamshell-like closure for preventing entry of seawater into the engine compartment (Fig. 3). This liquid-propellant booster was not developed further.[3] One reason given for NASA not considering a liquid-propellant SRB replacement, even after the loss of the Challenger, is that these boosters are more delicate than solid-propellant boosters and cannot withstand ocean impact and salt-water immersion.[4] The second design was a flyback booster (Fig. 4). This concept would require redesign of ET structure and attach points and major changes to the launch facility because of the new booster location; and the large added wing area would result in different aerodynamic characteristics during Shuttle launch.

Flyback Booster Concept Revisited

This paper proposes a flyback liquid-propellant booster to minimize recurring costs. The booster's wings and canard fins are stowed during launch, folded at their roots (Figs. 5 and 6). This was done to allow the LRB to use the same attach points on the ET as the SRB, minimizing the impact of the Shuttle's structure, ground facilities, and aerodynamics. State-of-the-art guidance and autolanding systems eliminate requirements for an onboard pilot. Maximizing the use of existing hardware and technology will reduce the booster's cost, risk, and development time, and follows the philosophy NASA used in developing the highly successful Saturn I booster in record time (Ref. 5, pp. 25–30 and pp. 323–337). The LRB design uses LH_2 and LO_2, the least polluting, most efficient propellant combination used to date.

LRB Mission Profile

The LRB was designed to provide a velocity increment to the Orbiter/ET/booster combination (stack) that exceeds that of the SRB, without violating Shuttle launch constraints such as 3-g maximum acceleration, or 700 lb/ft^2 (33.6 kPa) maxi-

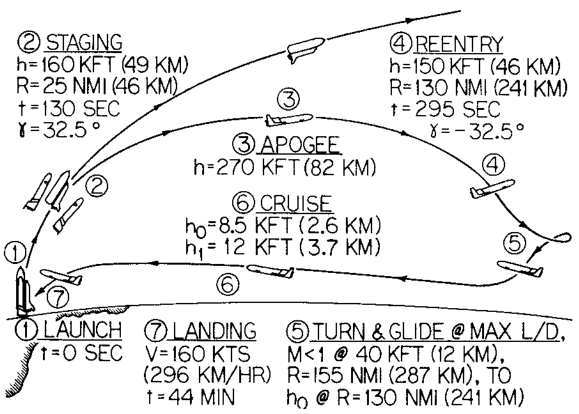

Fig. 7 LRB flight profile diagram.

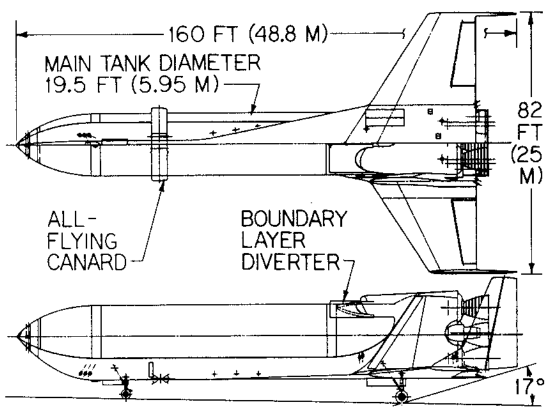

Fig. 8 LRB general arrangement, top and side views.

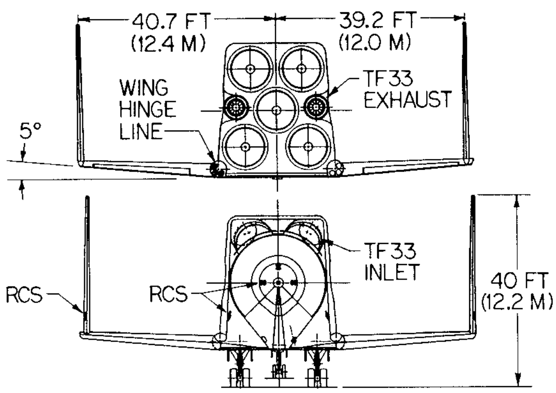

Fig. 9 LRB general arrangement, nose and tail views.

mum dynamic pressure. The 10 SSME's on the two strap-on LRB's burn in parallel with the 3 SSME's on the Orbiter until LRB propellant is exhausted at 126 s into the flight (Fig. 7). After staging at 160,000 ft (48.8 km) altitude, 25 n.mi. (46.3 km) downrange, each LRB coasts up to 270,000 ft (82.3 km) altitude in a ballistic trajectory, then re-enters the sensible atmosphere approximately 130 n.mi. (241 km) downrange.

Prior to re-entry, the LRB's wings and canard extend into flight configuration (Figs. 8 and 9). The LRB's attitude is controlled by its reaction control system (RCS) thrusters down to an altitude of approximately 100,000 ft (30.5 km) where its aerodynamic control surfaces begin to take effect. Residual RCS propellants are burned off prior to landing to reduce explosion and ground-handling hazards. The LRB re-entry speed of approximately 5000 ft/s (1524 m/s) is low enough that a special thermal protection system (TPS) is not required. The LRB's large aluminum tank and aluminum airframe is used as a heat sink, with its nose, leading edges, and other hot spots covered with titanium, as required. This "heat sink booster" concept is based on the structural design for the 1972 flyback booster (FBB) which would safely re-enter the atmosphere at the even higher speed of 6000 ft/s (1829 m/s) (Ref. 1, pp. 371-372).

During re-entry, the LRB makes a 180-deg turn as it decelerates to subsonic speed. The re-entry flight profile is based on predicted performance of the FBB, and the reduced entry speed of the LRB compared to the FBB should result in even less of a maximum load factor than the value of 3.2 predicted for the FBB. A subsonic lift-to-drag ratio (L/D) of 4.894 is estimated for the LRB, enabling a return glide distance of about 25 n.mi. (46.3 km) from turn completion at 40,000 ft (12,195 m) altitude to the initial cruising altitude of 8500 ft (2591 m). Two turbofan air-breathing engines (ABE's) with inlets and exhausts sealed at launch are provided for the 130 n.mi. (241 km) flight back to Kennedy Space Center's runway. The LRB could be flown either as a remotely piloted vehicle (RPV) or inertially like a cruise missile using the onboard automatic flight control system (AFCS).

Advantages of the LRB

This proposed LRB for the Space Shuttle would be fully reusable. The majority of its subsystems would be existing, qualified components used in the current Space Shuttle program. It would return intact to the launch site, eliminating the expense of ships, facilities, and personnel for ocean recovery. The technology for precise automatic navigation and flight control has been proven in cruise missiles, and an automatic landing system for the Orbiter was tested in 1971 (Ref. 1, p. 841). The expense, weight, risk, and operational complications of an onboard flight crew are, therefore, not necessary. An inherent ferry capability precludes the costly, time-consuming requirement of being ferried aboard a Boeing 747 or other specialized aircraft.

The LRB has no elaborate TPS to refurbish, and its five SSME's only fire for 126 s per flight, and so much less engine maintenance would be expected than on the Orbiter whose SSME's fire for 520 s per flight. Concerns about the reliability of the state-of-the-art SSME have been diminished as this engine has enjoyed a record of success (Ref. 6, p. 33) comparable to the successful large liquid-propellant engines used in the Saturn program. Since the LRB uses five current SSME's instead of four advanced engines, its lifting power can be upgraded when more powerful engines become available. The LRB, with a lower landing speed and weight than the Orbiter, would require fewer tire and brake replacements.[7,8] The advantages of return-to-launch-site and reduced refurbishment could add up to a much shorter turnaround time for the LRB compared to the Orbiter, and so a fleet of four Orbiters could probably get by with as few as four LRB's. After initial LRB development costs, which are mitigated by the use of existing components, the cost per Shuttle flight should be much lower than present.

Concerns have been raised about the long-term use of the SRB. The exhaust plume of the SRB releases HCl gas into the stratosphere, which could cause depletion of the ozone layer.[9] Damage to the ecology near the launch site could also occur from "acid rain." The LRB would minimize pollution of the upper atmosphere and the launch site, as the SSME exhaust is simply water vapor. The pace of Shuttle launching can only increase in the future, especially to support the Space Station, and so environmental pollution could be a growing concern. Most importantly, the LRB could make operation of the Space Shuttle safer. Liquid-propellant engines can be shut down at any time during ascent, making emergency fast separation of the Orbiter more feasible. At ignition the combined vehicle can be held on the pad until the computer verifieis proper operation of all of the engines. This has been demonstrated on Shuttle flights where SSME's were shut down prior to SRB ignition.

LRB Booster Preliminary Design

Structural and Main Propellant Tank Design

The LRB inboard profile views are shown in Figs. 10 and 11. Thrust loads from the five SSME's are transmitted to the aft end of the main propellant tank. Because the LRB has to transmit these loads to its forward end connection with the external tank under compression, an integral propellant tank, with a double-walled common bulkhead between the LH_2 and LO_2, was used for stiffness. An integral tank has the added advantages of being lighter, more streamlined, and shorter than a comparable two-tank design. Common bulkheads between cryogenic tanks were successfully used on the Saturn S-IV, S-IVB, and S-II stages (Ref. 5, pp. 167–168 and pp. 211–213). Stiffening-ring inserts are provided at three locations: at the SSME thrust structure/aft tank interface, at the common bulkhead, and at the forward tank barrel section/ET thrust structure interface.

The main propellant tank's nose is ogival to reduce drag, and the other two bulkheads are elliptical. Internal tank insulation, proven on the S-IVB stage (Ref. 5, pp. 172–177), is required in order to utilize the heat-sink re-entry concept. Insulation of the tank skin from cryogenic liquid propellants should also increase the tank's fatigue life. The small undertank fuselage provides buckling stiffness along the side of the tank connected to the Shuttle ET and houses the nose landing gear, RCS tankage, auxiliary power unit (APU) systems, canard control systems, and avionics, while allowing for thermal expansion and contraction of the main tank. Forward-locating auxiliary equipment helps to balance the large weight in the tail, minimizing the amount of ballast required to correctly position the CG for flight stability.

Main Propellant and SSME System

The much shorter LO_2 tank was placed aft of the LH_2 tank to minimize the weight of SSME feeder piping required to connect the forward tank to the engines. Two 17-in. (432-mm) LH_2 feeder lines connect the LH_2 tank with an LH_2 distribution manifold in the engine bay. One 17-in. (432-mm) feeder supplies the three Orbiter SSME's from the ET, and so two 17-in. (432-mm) feeders for five LRB engines should be adequate. Individual 12-in. (305-mm) LH_2 and LO_2 feeders connect each SSME to the LH_2 manifold and rear LO_2 tank sump.

The LRB's SSME's are gimballed in two degrees of freedom through ± 7 deg to equal the control power of the SRB nozzle. Other systems such as recirculation, pressurization, fill/drain, and venting lines use components that are the same as those used on the Orbiter/ET, as are all of the main feeder lines and valves. Propellant tank vents are spaced such that, when on the launch pad, the LH_2 vent discharges at the same level as the ET LH_2 vent and the LO_2 vent discharges at a sufficient distance below the LH_2 vent for separation of O_2 and H_2 vapors.

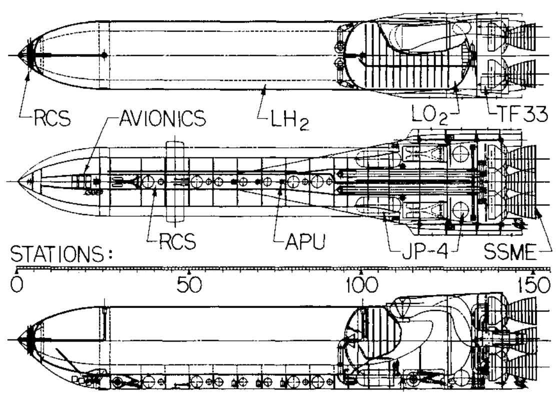

Fig. 10 LRB inboard profile, plan and elevation views.

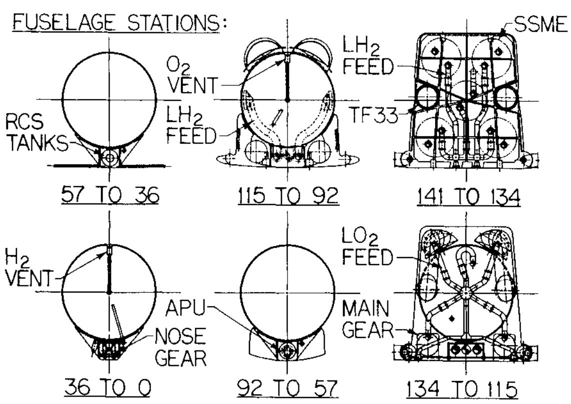

Fig. 11 LRB inboard profile, section views.

Booster Performance Calculations

The powered ascent from liftoff to booster separation was simulated by integrating an equation of motion using a Runge-Kutta routine with a preset tilting function curve-fit from previous Shuttle trajectories. Parameters for the SRB/ET/Orbiter trajectory model, such as drag coefficients, were obtained from Ref. 10. Actual Space Shuttle weights were obtained from Refs. 6–8, 11, and 12, and SSME data were obtained from Refs. 6 and 11. The LRB's SSME's mass flow rate (and thrust) were varied in a similar manner as on current Shuttle flights (100% for $0<t<9$ s, 104% for $9<t<48$ s, 65% for $48<t<63$ s, 104% for $63<t<117$ s, and 65% for $117<t<126$ s). The SSME mass flow rate used was 1130 lb_m/s (513.6 kg/s) at 100% thrust. The LRB/ET/Orbiter launch data used for integration initial conditions are summarized in Table 1.

The equation of motion and tilting function curve-fit are given by

$$dV/dt = T(t)/m(t) - g\cos\theta(t) - (0.5)\rho Vt^2 SC_d(t)/M(t) \quad (1)$$

$$\theta(t) = \tan^{-1}\{(1.5707)\sin[(1.5707)\{1 - \exp[-3.5(t/89)]\}]\} \quad (2)$$

Result: The LRB design provides a 10% higher velocity increment to the stack than the SRB at staging. LRB/SRB

Table 1 LRB launch data

LRB gross liftoff mass	850,000 lb_m	(386,364 kg)
LRB nonpropellant mass	150,000 lb_m	(68,182 kg)
Maximum payload mass	65,000 lb_m	(29,545 kg)
Orbiter mass	205,000 lb_m	(93,182 kg)
Maximum ET mass	1,655,000 lb_m	(752,273 kg)
2 LRB's at maximum mass	1,700,000 lb_m	(772,727 kg)
Combined max. liftoff mass	3,625,000 lb_m	(1,647,727 kg)
Combined max. thrust	4,875,000 lb_f	(21,738,070 N)
Thrust-to-weight ratio	1.345 (13 SSME's @ 100%)	

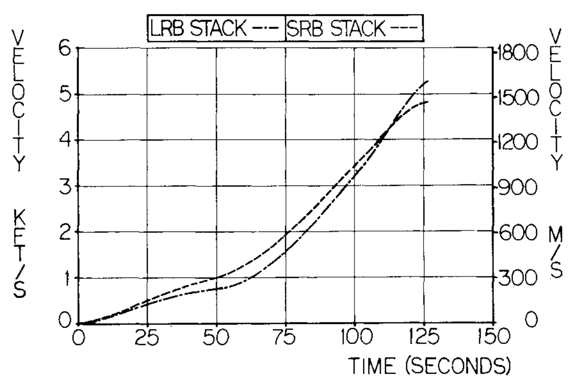

Fig. 12 Comparison of LRB and SRB performance, velocity magnitude.

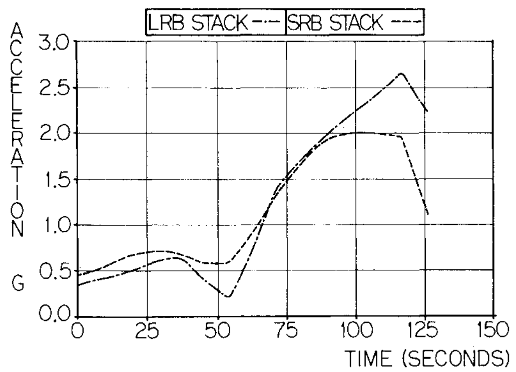

Fig. 13 Comparison of LRB and SRB performance, acceleration magnitude.

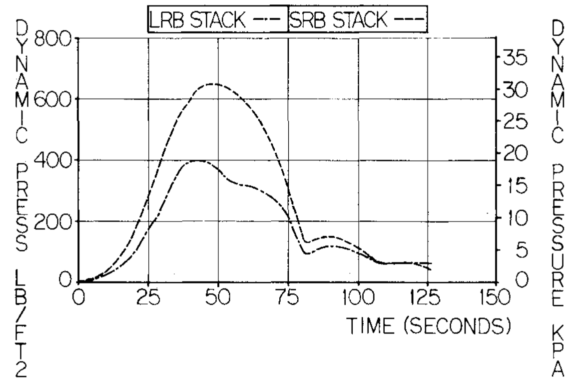

Fig. 14 Comparison of LRB and SRB performance, dynamic pressure.

comparison plots for velocity, acceleration, and dynamic pressure are shown in Figs. 12, 13, and 14, respectively.

Main Propellant Tank Sizing

The LRB main propellant tanks were sized using the Space Shuttle ET design data from Refs. 6 and 12 as a guide. Total propellant for the maximum load mission was 731,350 lb_m (332,432 kg), which includes 31,350 lb_m (14,250 kg) for 9 s of SSME thrust buildup to 100% thrust. Liftoff propellant is 700,000 lb_m (318,182 kg) including 14,000 lb_m (6364 kg) for 2.0% residuals at LRB shutdown and staging. Structural and insulation volume allowance was 2.5%, and ullage volume allowance was 5.0%.

Result: VLH_2 tank = 25,514 ft^3 (723 m^3), VLO_2 tank = 9494 ft^3 (269 m^3).

Booster Auxiliary Equipment

The LRB is provided with three hydrazine-driven APU/hydraulic pumps like those used on the Orbiter. They provide a double-redundant hydraulic system with pressure for SSME gimbal control, wing and canard deployment, flight control surface movement, landing gear control, and starting and control of the air-breathing engines.

The LRB is provided with six solid-propellant separation motors of the type used on the SRB, with three forward and three aft in the same general orientation as on the SRB. The separation motor cases are buried in the fuselage for a clean installation and can be placed on either side of the LRB so that the LRB's can be used on either the right- or left-hand side of the stack. Six motors should be adequate instead of eight as on the SRB, because the LRB is approximately 80% lighter at burnout than the SRB, and the drag on the LRB at separation is higher than on the SRB because of its higher reference area.

Two independent, three-axis attitude control systems, using the same tankage, primary thrusters, and propellants as the Orbiter aft RCS system, are provided for stabilizing the LRB from separation from the ET until after re-entry. Four pitch and four yaw thrusters are located in the nose of the LRB. Eight roll thrusters are located aft, two pairs on the fuselage, and two pairs on the wingtips. All eight roll thrusters can be used when the wings are stowed with the wingtip thrusters sufficing with the wings extended.

Table 2 Airfoil data

Characteristics	Wing	Horizontal	Vertical
Span, tail height, ft (m)	82 (25.0)	23 (7.01)	28 (8.54)
Reference area, ft^2 (m^2)	2320 (216)	115 (10.7)	784 (72.9)
Aspect ratio	2.898	4.600	4.000
Tip chord, ft (m)	14.6 (4.45)	5 (1.52)	8 (2.44)
Root chord, ft (m)	42 (12.8)	5 (1.52)	20 (6.10)
Mean aero. chord, ft (m)	30.5 (9.30)	5 (1.52)	15 (4.57)
Thickness, % chord	8	8	6
Sweepback at $c/4$, deg	26.6	0	12.7
Dihedral angle, deg	5	0	0.75
Incidence angle, deg	2	(variable)	0
Wetted area, ft^2 (m^2)	2828 (263)	265 (78.0)	1746 (532)

LRB Aerodynamic Preliminary Design

Wing and Canard Aerodynamic Design

The canard configuration was chosen because the weight of the five SSME's and two ABE's is concentrated near the tail, placing the CG at 74% of the reference body length of 147 ft (44.8 m). A NACA 1408 airfoil section was chosen for the wing primarily because of its low C_{mo} with adequate lift slope at a reasonable t/c for structural strength. The wing was designed to maximize aspect ratio within the constraints of reasonable wing loading [62.7 lb_f/ft^2 (3009 Pa) maximum], a maximum-folded dimension in relation to the ET and Orbiter, and positioning of the neutral point for static stability.

The variable-incidence (all-flying) canard employs a constant-chord NACA 0008 airfoil section, and its reference area is 5% of the wing reference area. Its position in relation to the wing-body aerodynamic center is such that the LRB will be longitudinally statically stable during supersonic glide and subsonic cruise. The equations of static longitudinal stability and balance, given by Ref. 13, Chap. 2, were rederived for the canard configuration and used to size and locate the canard fin using downwash parameters estimated from Ref. 14, p. 222:

$$C_{mo} = C_{mowb} + l_c S_c a_c/\bar{c}S\{[(1 - \partial\epsilon/\partial\alpha)i_c + \epsilon_o]/[(1 - \partial\epsilon/\partial\alpha) + a_c S_c/a_{wb} S]\} \tag{3}$$

$$C_{m\alpha} = -a_{wb}[(h_{nwb} - h)(1 - \partial\epsilon/\partial\alpha) - l_c S_c a_c/\bar{c}S a_{wb}] \tag{4}$$

Results: $C_{mo} = 0.010$, $C_{m\alpha} = -0.0033$/deg, with $i_c = 5$ deg.

Vertical Stabilizers and Rudders Aerodynamic Design

The twin vertical stabilizers, utilizing tapered NACA 0006 airfoil sections, are slightly offset from lateral symmetry to enable them to stow over-and-under with the wings folded. The aerodynamic characteristics of the Shuttle Orbiter were used as a guide in sizing the vertical stabilizers and rudders. The criteria were to obtain the same ratios of $C_{n\beta v}/C_{n\beta f}$ and $C_{n\delta v}/C_{n\beta}$ for static lateral stability (weathercock stability) and control (rudder power) as on the Shuttle Orbiter, using the procedure of Ref. 13, Chap. 3:

$$(C_{n\beta v})\max = (S_v l_v/Sb)a_v \tag{5}$$

$$(C_{n\delta v})\max = (S_v l_v/Sb)a_r \tag{6}$$

Results: $C_{n\beta v}/C_{n\beta f} = 0.032$, $C_{n\delta v}/C_{n\beta} = 0.030$, where the relation for $C_{n\beta f}$ was obtained from Ref. 13, p. 348. A summary of LRB airfoil data is given in Table 2.

Table 3 Mass statement, mass in lb_m (kg)

Equipment or assembly	Station	Empty	Consumable
8 nose RCS thrusters	4	400 (181.8)	—
Avionics and batteries	15	1,000 (454.5)	—
3 nose separation rockets	23	200 (90.9)	400 (181.8)
Nose landing gear assembly	32	1,200 (545.5)	—
Canard, hinge mechanism, actuators	46	1,200 (545.5)	—
RCS propellant, pressurization tanks	65	600 (272.7)	3,500 (1,591)
Forward fuselage, below main tank	70	10,200 (4,636)	—
3 APU/hyd. units, tanks, hyd. system	79	4,000 (1,818)	700 (318.2)
Main tank, piping, insulation	80	33,000 (15,000)	—
2 forward JP-4 tanks, nominal load	105	800 (363.6)	11,900 (5,409)
2 main landing gear assemblies	118	4,300 (1,955)	—
8 aft RCS thrusters	125	400 (181.8)	—
2 ABE ducts and duct closures	125	1,500 (681.8)	—
Wing, hinge mechanism & actuators	125	14,000 (6,364)	—
2 aft JP-4 tanks, nominal load	129	200 (90.9)	3,100 (1,409)
Thrust structure, fairing, heat shield	135	3,000 (1,364)	—
5 SSME's, 2 ABE's, engine controls	141	43,600 (19,818)	—
3 aft separation rockets	141	200 (90.9)	400 (181.8)
2 vertical stabilizers	148	4,000 (1,818)	—
Design margin of 5%	90	6,200 (2,818)	—
Weight totals	—	130,000 (59,091)	20,000 (9,091)

Weight Estimation

Component weights for the LRB were estimated from previous launch vehicles if an exact component weight could not be obtained. The LRB main propellant tank weight was estimated from the Shuttle ET weight and other propellant tank studies contained in Ref. 1. Wing, fuselage, and stabilizer weight were estimated using current aircraft design practice. A 15% weight allowance was added to the wing and canard weights to account for the folding actuators, hinges, and associated equipment. Data in Refs. 1-3 and 5 concerning various existing or studied launch vehicles and components were also used for weight estimation, which is summarized in Table 3.

Aircraft Flight Performance

The following calculations are examples of some of the analyses done to determine the LRB's aircraft flight performance and size the turbofan ABE's and JP-4 tanks. The zero-lift drag coefficient C_{do} was estimated to be 0.085 using the procedure of Ref. 15, Chap. 3. A large contribution was due to base drag C_{db}, estimated to be 0.034, and the large fuselage wetted area of 10,700 ft^2 (995 m^2). The Oswald efficiency factor e was estimated to be 0.775. Aspect ratio A is effectively increased from 2.898 (geometric) to 3.345 by the end-plate effect of the vertical stabilizers as shown in Ref. 16, pp. 3-9. The following performance calculations were made in accordance with Ref. 17, Chap. 6, and Ref. 18. At $(L/D)_{\max}$

$$C_l^2/\pi Ae = C_{do} \tag{7}$$

$$C_d = 2C_{do} \tag{8}$$

Results: $C_l = 0.832$, $C_d = 0.170$, $(L/D)_{\max} = 4.894$; maximum range occurs at

$$(C_l^{1/2}/C_d)_{\max}$$

where

$$C_{do} = 3C_l^2/\pi Ae \tag{9}$$

Results: $C_l = 0.480$; with a cruise-climb return, holding C_l constant, and $h_0 = 8500$ ft (2591 m), $W_0 = 145{,}500$ lb_m (66,136 kg); $h_1 = 12{,}000$ ft (3659 m), $W_1 = 130{,}500$ lb_m (59, 318 kg), range is given by

$$R = 2[2/\rho S]^{1/2}(1/c)(C_l^{1/2}/C_d)_{\max}[W_0^{1/2} - W_1^{1/2}] \tag{10}$$

Results: $R = 150$ n.mi. (277.9 km). With $L = W$, cruising speed is given by

$$V_c = [W/(0.5)\rho SC_l]^{1/2} \tag{11}$$

Results: $V_c = 216$ knots (400 km/h) at h_0, 228 knots (422 km/h) at h_1. The thrust required at beginning and end of cruise is given by

$$T_r = D = (0.5)\rho V_c^2 S(4/3)C_{do} \tag{12}$$

Results: $T_r = 34{,}000$ lb_f (151,600 N) at h_0, 30,470 lb_f (13,870 N) at h_1.

Air-Breathing Engines and Auxiliary Equipment

Two Pratt & Whitney TF33 (commercial designation JT3D) turbofans were selected for the LRB to satisfy the calculated T_r. During ascent and re-entry, the engine inlets are covered by streamlined, hydraulically actuated clamshell fairings that open as part of the engine-starting sequence. The engine exhaust ducts are covered by heat-shield fairings to prevent damage to the ABE's during firing of the SSME's. These fairings are jettisoned from the LRB prior to engine starting. Hydraulic accumulators charged by the APU-driven hydraulic system are used to start the engines. Internal fuel tankage is designed to accommodate up to 20,000 lb_m (9091 kg) of JP-4 in four pressurized propellant tanks arranged such that the CG of the LRB will not shift with a balanced fuel withdrawal from forward and aft tanks.

The LRB uses the same landing gear as the Shuttle Orbiter. This landing gear can be released by pyrotechnics and lowered and locked by gravity in the event of a hydraulic system failure. The current Orbiter landing gear has no provision for retraction during flight after it has been lowered, and so a retraction mechanism would have to be provided, along with additional fuel tanks if an extended-range ferry capability is desired for the LRB.

In addition to the telemetry and range safety systems carried on the SRB, inertial navigation and automatic flight control systems, similar to those used in cruise missiles, are also included on the LRB. A wide-angle television camera is provided for remote piloting if automatic landing is not desired. The avionics systems are powered by batteries during the short-duration launch, re-entry, and recovery flight.

Conclusion

The objective of this paper has been to present a design for a more capable, environmentally acceptable, and safer Shuttle booster. The flyback feature would reduce recurring cost, and development time and cost could be reduced by maximizing the use of existing hardware and proven technology. The folding-wing feature would minimize impact to existing Shuttle components and ground facilities, and five engines provide future growth in lifting capacity. The propellants chosen would minimize atmospheric and launch site pollution and offer more options for aborting a mission both on the pad and during the boost phase. The reusable flyback liquid rocket Booster could be a logical next step in the evolution of the U.S. Space Transportation System.

Acknowledgments

This paper, plus analysis and drawings, were done in partial fulfillment of requirements for the degree of Master of Science. The author would like to thank his advisor, Dr. John D. Anderson Jr., and the faculty and staff of the University of Maryland Department of Aerospace Engineering, for their advice, assistance, and encouragement in this independent research project.

References

[1] *Space Shuttle-Skylab, Manned Space Flight in the 1970's,* U.S. House of Representatives Status Report, Subcommittee on NASA Oversight, U.S. Government Printing Office, Washington, DC, Jan. 1972.

[2] *Space Shuttle-Skylab, 1973,* U.S. House of Representatives Status Report, Subcommittee on NASA Oversight, U.S. Government Printing Office, Washington, DC, Jan. 1973, pp. 1,2.

[3] *Space Shuttle 1979,* U.S. House of Representatives Status Report, Subcommittee on NASA Oversight, U.S. Government Printing Office, Washington, DC, Jan. 1978, pp. 572–586.

[4] DeMeis, R., "Shuttle SRB: NASA's Comeback Bid," *Aerospace America,* Vol. 25, No. 4, April 1987, pp. 32–38.

[5] Bilstein, R. E., *Stages to Saturn, A Technological History of the Apollo-Saturn Launch Vehicles*, NASA SP-4206, 1980.

[6] Robinson, J. W. (ed.), *Shuttle Propulsion Systems*, American Society of Mechanical Engineers, New York, Nov. 1982.

[7] Felder, G. L., "The Space Shuttle Program, From Challenger to Achievement, Space Exploration Rolling on Tires," *Proceedings of NASA JSC Space Shuttle Technical Conference*, NASA CP-2342 Pt. 2, Jan. 1985, pp. 857–860.

[8] Carsley, R. B., "Space Shuttle Wheels and Brakes," *Proceedings of NASA JSC Space Shuttle Technical Conference*, NASA CP-2342 Pt.2, Jan. 1985, pp. 872–879.

[9] Averner, M. M. and MacElroy, R. D., "Speculation on the Consequences to Biology of Space Shuttle-Associated Increases in Global UV-B Radiation," NASA TM-X-73200, Jan. 1977, pp. 1–159.

[10] "STS-1 Operational Flight Profile," Vol. 3, Ascent, NASA TM-81096, May 1980.

[11] *The Space Shuttle Main Engine*, Rockwell International, Rocketdyne Div., Canoga Park, CA, Pub. 574-E-4, Nov. 1985.

[12] *External Tank Fact Sheet*, Martin Marietta Corp., Michoud Div., New Orleans, LA, Pub. 0327M, Nov. 1987.

[13] Etkin, B., *Dynamics of Flight*, Wiley, New York, 1982.

[14] Perkins, C. D. and Hage, R. E., *Airplane Performance, Stability, and Control*, Wiley, New York, 1949.

[15] Roskam, J., *Methods of Estimating Drag Polars of Subsonic Airplanes*, Univ. of Kansas, Lawrence, KS, 1971.

[16] Hoerner, S. F. and Borst, H. V., *Fluid Dynamic Lift*, Hoerner Fluid Dynamics, Brick Town, NJ, 1975.

[17] Anderson, J. D., Jr., *Introduction to Flight*, McGraw-Hill, New York, 1985.

[18] *JT8D-11 (TF33) Engine Specification*, Pratt & Whitney Aircraft Co., East Harford, CT, Aug. 1974.